

**Babeş-Bolyai University
Faculty of Physics**



Ph.D Thesis Summary

Characterization, detection and monitoring of harmful substances in food, using Raman spectroscopic techniques

MÜLLER Csilla

**Advisor
Prof. Dr. Leontin DAVID**

**CLUJ-NAPOCA
2013**

Keywords: *food additives, thiabendazole, citrus fruits and bananas, marine toxin, domoic acid, fish tissue, Raman, SERS.*

CONTENTS

INTRODUCTION.....	4
CHAPTER I. The importance of research and the state of the art in the detection, monitoring and characterization of harmful substances in food..	5
I.1. Food quality control, and the current issues in the field	5
I.2. Vibrational techniques in food quality control	6
I.2.1. Raman Spectroscopy	6
I.2.2. SERS Spectroscopy (Surface Enhanced Raman Spectroscopy).....	7
I.2.3 The role of theoretical methods in the field. Basic principles of DFT methods	8
Chapter II. Vibrational techniques applied for controlling and monitoring fruit quality	9
II.1 Food Additives - Why are they necessary?	9
II.2 The case study: thiabendazole (E 233)	9
II.2.1. The Raman spectrum of thiabendazole	10
II.2.2. The SERS spectrum of thiabendazole adsorbed on silver colloidal nanoparticles	11
II.2.2.1. The concentration dependence SERS spectra	12
II.2.2.2. The pH dependence SERS spectra.....	13
II.2.3. SERS detection of thiabendazole in citrus fruits.....	14
II.3. Conclusions.....	16
CHAPTER III. Vibrational characterization and monitoring of biotoxins in aquaculture products.....	17
III.1. Marine biotoxins.....	17
III.2. Domoic acid	18
III.2.1. The Raman and SERS spectra of seawater	18
III.2.2. The Raman and SERS spectra of water from aquaculture.....	19
III.2.3. The FT -Raman spectrum of domoic acid	20
III.2.4. The SERS spectrum of domoic acid	20
III.2.4.1. The concentration dependence SERS spectra of domoic acid in pure water and seawater	21
III.2.4.2 The SERS signal of domoic acid on amino - functionalized silver nanoparticles.....	22
III.2.4.3 SERS detection of domoic acid in fish tissue	24
II.3. Conclusions.....	26
REFERENCES	
PUBLICATIONS	

INTRODUCTION

The thesis is divided into three chapters. The first chapter describes the importance of research in finding techniques for detecting, monitoring and characterization of toxic substances in food control and are briefly described the experimental methods (FT-Raman, SERS) and theoretical methods (DFT), used to determine the investigated species in the experimental part of this thesis.

The second chapter deals with the food additives and is focused on the physico-chemical characterization of the tiabenedazole (TBZ) molecule. This food additive has been investigated in solid state and in water and ethanol solutions by Raman and SERS spectroscopy. Using DFT methods it has been obtained the molecular geometry optimization and calculation of vibrational frequencies. Known as E233 in Europe, thiabendazole is widely used as a preservative in food industry, for fruits and vegetables. It is shown that TBZ can be quickly detected by Raman spectroscopy (at millimolar concentration) and SERS (from micro- to picomole level using silver colloidal nanoparticles and a compact portable, mini – Raman spectrometer. The vibrational data were used to detect TBZ from treated citrus and bananas.

The third chapter contains original results obtained by the study of some biotoxins that appear in areas of aquaculture and which can get into fish and other marine products. Detailed studies are focused on domoic acid molecule. This study represents a combination of obtained experimental results by using vibrational spectroscopic methods with results from literature. This natural neurotoxin has been characterized and detected by SERS method, both in pure water and seawater. Three different schemes for detection of domoic acid in seawater have been described by dissolving the crystalline acid in seawater, by diluting pure water with seawater or by using functionalized nanoparticles (animo-AgNPs). Specificity of dependence of signal of the used method has been discussed in all cases. This section demonstrated the orientation and the adjustment of domoic acid to the metal surface and the detection of these marine toxins in seawater, respectively in fish tissue, using SERS technique, at lower concentrations than currently used methods.

CHAPTER I. The importance of research and the current state of the art in detection, monitoring and characterization of harmful substances in food

I.1. Food quality control and current issues in the field

In all countries, the food industry has the responsibility to fulfill the conditions on food quality and safety regulatory requirements. Supply chains can be as short as the garden is from the family table, or thousands of miles long, with many intermediates. The systems of conservation, the processing and packaging of the food products can be minimal or very sophisticated, but to ensure food quality and safety, in all situations must be constant. The industry must play its role in ensuring food quality and safety by applying quality assurance and food safety systems based on risk, using current scientific knowledge. The implementation of such controls throughout production, handling, processing and marketing leads to quality improvement and food safety, increasing competitiveness and reducing production costs and waste. [1]

Rapid analysis of the chemical composition is of major importance. The main techniques in use by the control and monitoring food products are: Liquid chromatography (LC), [2-4] gas chromatography coupled with mass spectrometry (GC-MS), with the addition of micro-biological analyzes, and classic physico-chemical analyzes (density, pH, color, concentration) and organoleptic. These technologies cover broad areas of analysis, but these techniques are expensive, require significant time for sample preparation and relatively long analysis, being related to the laboratory.

Raman spectroscopy has taken a real momentum nowadays over other methods for monitoring chemical reactions, pharmaceutical and chemical food analyzes and also for various other everyday applications. Raman spectroscopy offers detailed information on molecular vibrations. Whereas these vibrations depend on the strength and type of chemical bonds, Raman spectroscopy is useful not only to identify but also in the study of molecules and intermolecular interactions. Vibrational spectroscopy is used to elucidate the structures and physico-chemical properties of the compounds investigated.

Concerns (especially in recent years) on food analysis requires the development of rapid and accurate methods for the determination of food additives and toxic substances, and one of these methods can provide vibrational spectroscopy in particular through its branch Surface-enhanced Raman Spectroscopy (SERS).

I.2. Vibrational techniques in food quality control

I.2.1. Raman Spectroscopy

Raman spectroscopy is based on the phenomenon of scattering of light in the UV-VIS and near infrared range. Raman spectroscopy is a nondestructive technique that can be applied on solid substances, liquids or gases, but it is a "weak" process, the scattering cross section is 10^{-31} - 10^{-26} cm²/molecule.

If, on the molecule falls an electromagnetic wave, the molecule size is smaller compared to the wavelength of the radiation, the of wave's electric field acting on electrons of the molecule, moving from the position of equilibrium. Arises an induced dipole moment μ , which in a first approximation is given by the relation:

$$\vec{\mu} = \alpha \vec{E}$$

, in which α is the polarizability tensor, depends on the structure and the nature of molecular bonds, E is the electric field intensity of the incident wave.

$$\mu_i = E_i^0 \left\{ \alpha_i^0 \cos 2\pi\nu_0 t + \sum_{k=1}^{3N-6} \left(\frac{\partial \alpha_i}{\partial q_k} \right)_0 q_k^0 \left[\frac{1}{2} \cos 2\pi(\nu_0 + \nu_k) t + \frac{1}{2} \cos 2\pi(\nu_0 - \nu_k) t \right] \right\}$$

It is noted that the dipole moment varies in time, which results an emission of radiation with a frequency ν_0 – difussion Rayleigh, with a frequencies $(\nu_0 + \nu_k)$ - difussion anti-Stokes Raman and with $(\nu_0 - \nu_k)$ – diffusion Raman Stokes. [5-12]

1.2.2. SERS Spectroscopy (Surface Enhanced Raman Spectroscopy)

The SERS Spectroscopy due to the amplification of Raman signal has become one of the most used techniques in the study of adsorbed molecules. For obtaining the SERS phenomenon the support is nanometer rough metal, the most used metals being silver, gold and with less extent, copper.

The intensity of the normal Raman scattering for a free molecule, is determined by the induced dipole moment of the transition μ , which is depend on the intensity of the electric field, E and the polarizability of transition α ($\mu = \alpha E$). SERS can be determined or by the increasing electric field or by the increasing of the polarizability, and hence becomes two different basic theories for explaining mechanism of the amplification:

- electromagnetic theory, that involves increasing the electric field at the place where the molecule is adsorbed
- the chemical theory, which involves the increase of the polarizability due to the formation of a complex molecule-metal, which will present a new absorption band compared to unadsorbed molecule in the frequency range of radiation excitation, namely it will induce a resonant Raman phenomenon after adsorption.

In the case of SERS the adsorbed molecules are both under the influence of the electric field radiation as under the plasmonic field. The Raman Stokes lines of the molecule are also close to the frequency of the excitation radiation, they will also be in resonance with the surface plasmon. For SERS signal intensity we can write:

$$I_{SERS} = N' I(\nu_L) |A(\nu_L)|^2 |A(\nu_S)|^2 \sigma_{SERS}^R$$

where N' - number of the adsorbed molecules, $I(\nu_L)$ - intensity of the excitation laser radiation, ν_L , $|A(\nu_L)|^2$ the intensity of excited plasmonic field of excitation radiation, $|A(\nu_S)|^2$ the intensity of excited plasmonic field of Stokes radiation, ν_S , σ_{SERS}^R SERS scattering section, which is higher than the normal Raman scattering. [11-20]

1.2.3. The role of theoretical methods in the field. Basic principles of the DFT methods

For a proper understanding of Raman spectrums is essential to secure the award of all bands in the experimental spectra. For this purpose, methods of molecular quantum mechanics provides complementary data to those obtained experimentally. Correlation of theoretical results with those obtained by experimental spectroscopic aims to determine the exact molecular structures, molecular properties and an accurate analysis of Vibrational spectrums. A very good correlation between normal modes of experimental and calculated vibration gives us the security of a proper assignment of vibration frequencies.

Within the DFT methods in different combinations functional parts and correlation are are commonly used. Among them, the combination of B3LYP is used most often because proved skills in reproducing several molecular properties, including vibrational spectra. It was shown that the combined use of the functional B3LYP with the basis set 6-31G standard (d) represents an excellent compromise between accuracy and computational efficiency in the calculation of vibrational spectrums for large and medium molecules. [21-24]

Chapter II. Vibrational techniques applied for controlling and monitoring fruit quality

II.1. Food additives – Why are they necessary?

Through food additive "is meant any substance, which normally it is not consumed as a food in itself and which normally is not used as a characteristic ingredient of food consumption, whether or not have nutritive value, the addition intentionally of it in food for a technological purpose in the process of manufacturing, preparation, treatment, packaging, transport or storage of such food results, or is likely to result to have direct or indirect result of its transformation or its by-products in a component of such foods. " Food additives are authorized at EU level for all fifteen Member States, as well as Norway and Iceland.

In the European Union are stabilized the maximum quantities of certain food additives, which a manufacturer can use to conserve, store, in order to improve the quality of a food, etc. EU decided, that each authorized additive needs to be signaled on the label or on the package with the well known code: E number. The decision was taken in the idea of having a very precise legislation and regulation of additives and to facilitate informing consumers. [25-27]

II.2. The studied case: Thiabendazole (E233)

Thiabendazole (TBZ), [2-(4-thiazolyl) benzimidazole, $C_{10}H_7N_3S$, also known as E233 in Europe], is a chemical fungicide species and parasiticide largely used in vegetables and fruits treatment to prevent mold, blight, and other diseases resulting from long transportation and deposit. For example it is largely applied to bananas in order to ensure freshness, and it is a common ingredient in the waxes applied to the skins of citrus fruits. TBZ is supposed only to be. [28]

The Romanian Directive aligned to the EU regulation, provides the maximum level is 6 mg/kg, in the case of citrus fruits (orange, pomelo, grapefruit, lemon, mandarin), and 2 mg/kg for bananas [8, 9]. It is not approved as a food additive in the EU [10].

II.2.1. The Raman spectrum of thiabendazole

FT-Raman spectrum of solid polycrystalline TBZ is displayed in comparison with the theoretical spectrum in *Fig.1*. for the high and low wavenumber range, respectively in *Fig.2*. A very good correlation between the normal modes of experimental and calculated vibration modes gives us the security of a correct assignment of vibration frequencies.

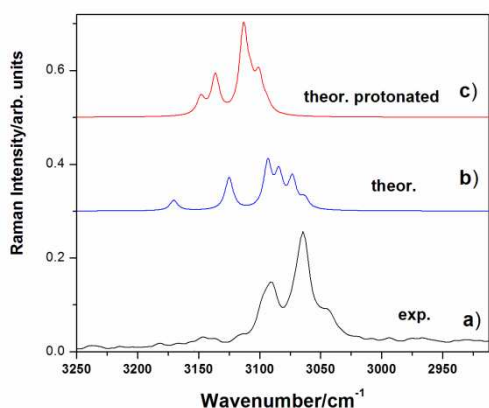


Fig.1. The experimental Raman (a) and theoretical (b) spectra of TBZ. A protonated form theoretically calculated spectrum (c) is given to support the experimental data of TBZ in aqueous solution in high wavenumbers range. Excitation (a): 1064 nm, 350 mW..

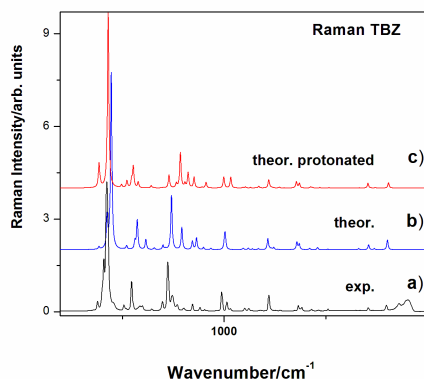


Fig.2. The experimental Raman (a) and theoretical (b) spectra of TBZ. A protonated form theoretically calculated spectrum (c) is given to support the experimental data of TBZ in aqueous solution in low wavenumbers range. Excitation (a): 1064 nm, 350 mW..

Fig. 3 present a series of Raman spectra of TBZ in aqueous solutions at two different concentrations, 10^{-3} and 10^{-2} mol l^{-1} respectively, and different pH values.

The Raman spectrum of TBZ aqueous solution at pH7 presents the same band positions (in the limit of solvent effect of 2-3 cm^{-1}) as the solid TBZ, while the spectra at pH4 and pH 2 exhibited different shape. Tus, the band at 1579 cm^{-1} is decreased at pH 4 and completely disappears at pH2. Instead, a new band centered at 1601 cm^{-1} was observed, whose intensity increased with pH decreasing. We suppose that probable a protonation at N atom from ring 2 is responsible for the new observed band at

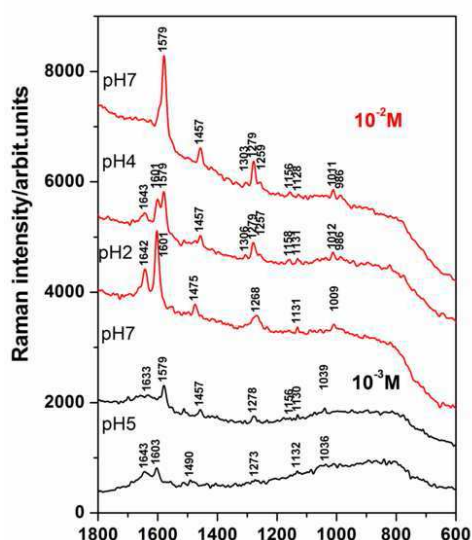


Fig.3. pH dependence Raman spectra of TBZ in aqueous solutions at two different concentrations, 10^{-2} (black) and 10^{-3} mol l^{-1} (red spectra), respectively. Excitation: 532 nm, 40 mW

1601 cm^{-1} . The same assumption was made for the second N atom (ring 1) since we observed another increasing band with pH decreasing at 1634 cm^{-1} , the $\delta(\text{N-H})$ bending mode after protonation. The shift of the band at 1279 cm^{-1} from the Raman spectra of neutral.

Concluding, a rapid measurement using a portable Raman instrument allowed to evidence in TBZ aqueous solution at $10^{-2} \text{ mol l}^{-1}$ two distinct species, the neutral and the protonated one respectively. The protonation behavior as revealed by the Raman spectrum is the same at $10^{-3} \text{ mol l}^{-1}$ concentration, although the normal Raman signal is very weak. However, this concentration range is unsatisfactory for sensitive detection applications. Therefore, we employed SERS to establish the optimal algorithm for trace detection of TBZ.

II.2.2. The SERS spectra of thiabendazole adsorbed on silver colloidal nanoparticles

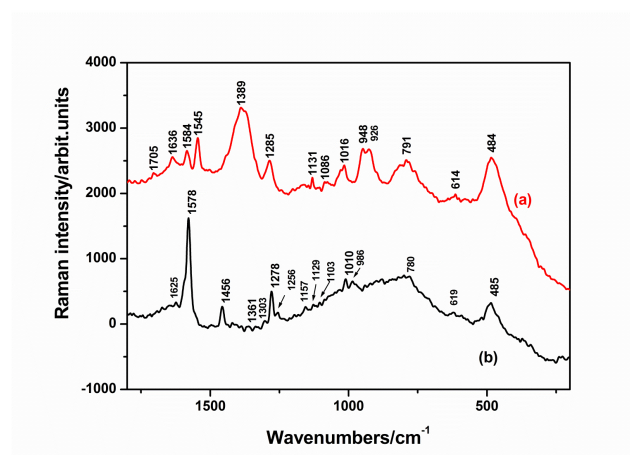


Fig.4. SERS spectrum of TBZ (a) in comparison with Raman spectrum (b) in aqueous solution. Excitation: 532 nm, 40 mW.

SERS spectrum of TBZ is presented in the *Fig. 4* in comparison with the Raman spectrum of aqueous solution at pH 7.

The SERS signal of the TBZ aqueous solution at $1.96 \cdot 10^{-5} \text{ mol l}^{-1}$, pH7 exhibits strong differences in band positions and relative intensities, when compared to the Raman one at $10^{-2} \text{ mol l}^{-1}$, suggesting a chemisorption process. Theoretically, the TBZ species could

adsorb through lone pair electrons from N or S atom (or both) resulting in a standing-up orientation to the Ag nanoparticles surface, or through the π ring electrons resulting a planar coverage of the surface.

The broadening of the bands strongly shifted when compared to the normal Raman ones, suggests a tilted to parallel orientation of the molecular skeleton with respect to the Ag surface.

II.2.2.1. Concentration dependence SERS spectra of TBZ

SERS detection limit of TBZ in aqueous solution using the mini-Raman spectrometer as 10^{-11} mol l^{-1} concentration. (Fig.5). The relative intensity of the band at 1389cm^{-1} (representative for TBZ concentration variation) versus 484cm^{-1} , I_{1389}/I_{484} as a function of concentration is displayed in insertion

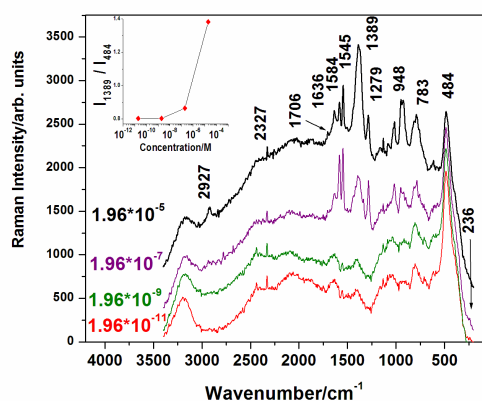


Fig.5 The concentration dependence SERS spectra of TBZ from micromole to picomole level, as shown on each spectrum.

A better SERS approach revealed the TBZ dissolved in ethanol, as shown in the Fig.6, where the concentration range for detection limit is higher with about three orders of magnitude.

The prominent SERS signal was still obtained at 6.65×10^{-14} mol l^{-1} and the sample was still SERS active even after 24 hours from preparation. The higher concentration ($6.67 \mu\text{mol } l^{-1}$) strongly activated the aggregation of the nanoparticles which results in visible macro-aggregates at the bottom of sample and

consequently, the diminishing of the absolute SERS intensity in time (Fig.6, right).

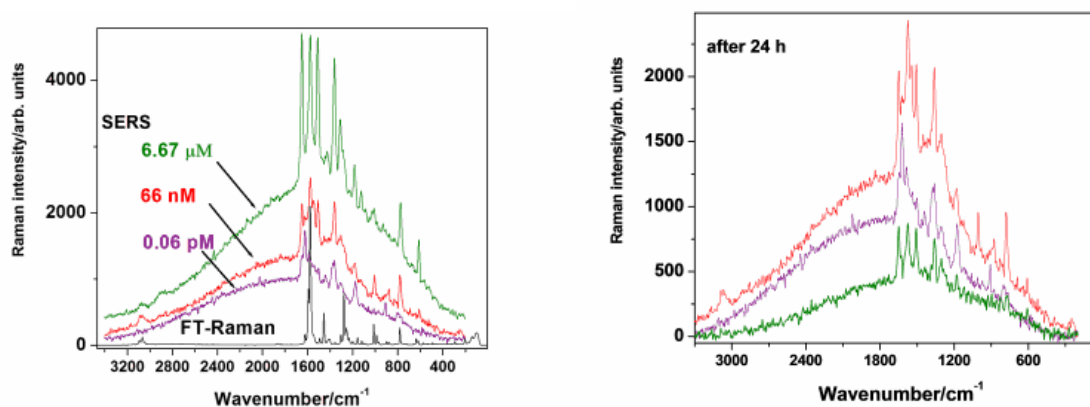


Fig.6. . Concentration dependence SERS spectra of the TBZ-ethanol solution, as indicated on each spectrum (left). The same samples exhibit strong SERS signal even after 24 hours (right), although at higher concentration the nanoparticles aggregation in the presence of TBZ is faster and consequently, the absolute SERS intensity is dramatically decreased to one half, from about 4000 to 2000 counts.

Excitation: 532 nm, 40 mW.

We employed even the 1064 nm laser line to probe FT-SERS using a near-infrared laser line, at 1064 nm (Fig. 7). Very sharp bands were observed at 6.67×10^{-6} mol l⁻¹ concentration.

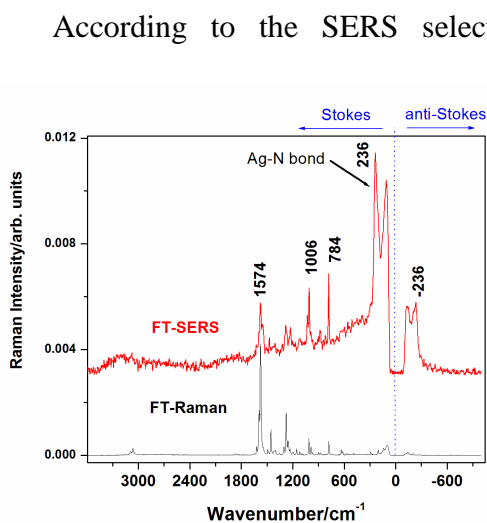


Fig.7. FT-SERS spectrum of TBZ – ethanol solution at 6.67×10^{-6} mol l⁻¹ concentration compared to the FT-Raman spectrum.

ethanol solution.

SERS signal of TBZ-ethanol solution (Fig. 8) as well as the FT-SERS experiment (Fig. 7) confirmed the chemisorption of ethanol-dissolved TBZ through both N and S atoms, resulting a standing-up orientation of the TBZ skeletal plane with respect to the Ag nanoparticles surface.

II.2.2.2. The pH dependence SERS spectra of TBZ

As expected, at basic pH range the SERS spectral shape (not shown here) is changed, probably because of the interaction with the citrate ions from Ag colloidal solution. The absolute signal intensity is much lower than in the acid media. (Fig.8)

The most significant SERS bands in the acid pH range are much better resolved than in the basic

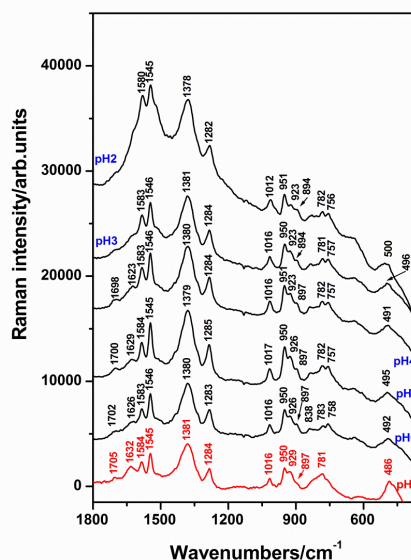


Fig.8. The pH dependence SERS spectra of

TBZ in acid pH range.

Excitation: 532 nm, 40 mW.

conditions (Fig. 8).

The relative intensity of the 1584 cm^{-1} and 1545 cm^{-1} bands are changed with pH decreasing.

According to the SERS selection rules [30], the spectral shape suggests that the protonated TBZ species adsorbs through the N or S (or both) from ring 1, resulting a torsion skeletal plane along the $-\text{C}-\text{C}-$ bond axis between ring 1 and 2, and co-existing different tilted orientations skeletal planes with respect to the Ag surface. The co-existence of both protonated and neutral species could not be excluded.

In addition, the protonated species supposed from the Raman spectra of aqueous solution confirmed by the theoretical calculated spectrum, revealed the new N-H bands after protonation at 1643 cm^{-1} which was observed in the SERS spectra as a strong shoulder at pH 2, whereas at pH above 4, a slight shift in the 1705 cm^{-1} – 1698 cm^{-1} range appears.

II.2.3. SERS detection of TBZ in fruits

The fruit samples (orange, lemon, banana, grapefruit and bio-lemon) have been randomly selected from market, domestic washed with tap water and prepared by immersing a small piece of peel in 100 ml distilled water. $10\text{ }\mu\text{l}$ from the resulted water solutions were used for SERS measurements.

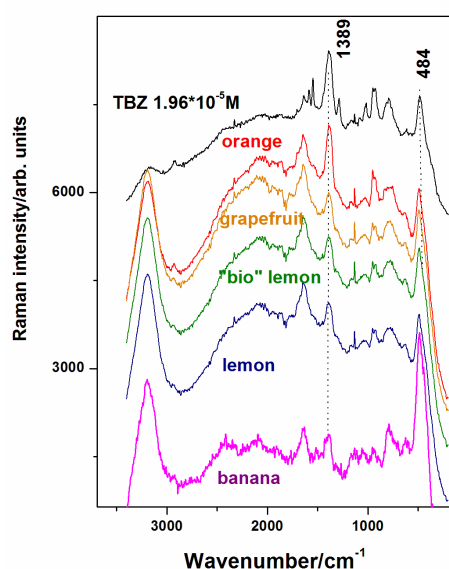


Fig.9. SERS spectra of TBZ collected from fruits compared to SERS signal of TBZ $10^{-5}\text{ mol l}^{-1}$.
Excitation: 532 nm, 40 mW.

The SERS signal of TBZ at pH 7 was successfully identified in the water samples resulted after immersion of the bananas and the four different citrus fruit species, including the “bio” lemon acquired from a specialized “bio” shop. (Fig.9) Water samples after 15 min, 30 min, 1h and 24h of fruit immersion were also investigated in a time dependence experiment (Fig.10). After 15 min of fruit immersion in water, the TBZ was detectable in the solutions. Longer immersion time resulted in higher SERS signal. Taking into account the SERS concentration dependence specificity, the typical SERS signal of neutral TBZ at $10^{-5}\text{ mol l}^{-1}$ was identified in the samples from 24 h immersion,

including “bio” lemon. This result is supported by the relative intensity ratio r of the observed bands I_{1389}/I_{484} that has values $r > 1$ only for $10^{-5} \text{ mol l}^{-1}$ concentration, whereas for lower concentrations, this ratio is $r < 1$. The results clearly evidenced that domestic washing fruit does not completely removed the TBZ content, since higher concentration signal detection was achieved from sample after longer water immersion time. Only in the case of TBZ extracted from banana this ratio is $r < 1$ which suggests a much lower concentration (most likely $1.96 \times 10^{-9} \text{ mol l}^{-1}$). Among citrus fruits, the orange revealed the highest TBZ level.

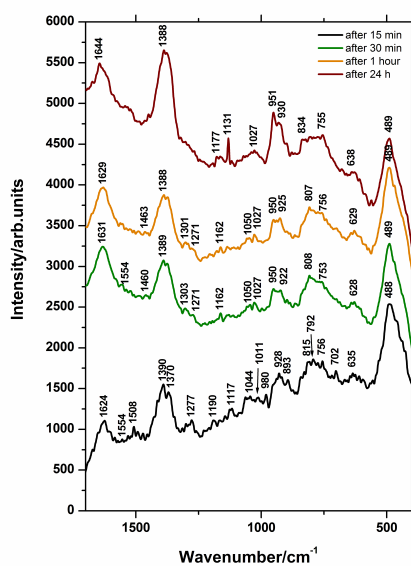


Fig.9. SERS signal collected from water resulted after fruits water immersion for 15 min, 30 min, 1 hour and 24 hours, as indicated from bottom to top, respectively.

Excitation: 532 nm, 40 mW.

(orange, pomelo, grapefruit, lemon, mandarin), and 2 mg/kg for bananas [29], since the total amount of fruit used in experiment was one small piece of peel of about 5 g, which provided approximately 78 mg/kg.

The SERS signal from fruit immersion solutions revealed the same bands as in the SERS spectrum of TBZ in neutral form, although some other small signal contributions from the complex sample in the $1545 \text{ cm}^{-1} - 1640 \text{ cm}^{-1}$ range was observed together with a higher Raman background resulted from other possible “impurities” from the fruits. However the TBZ has been unambiguously detected within 8 seconds measurement in all the studied cases. Taking into account the TBZ molecular weight of 201.249 g/mol, and the amount of $10 \mu\text{l}$ used as SERS sample volume, we could easily estimate for the concentration of $1.96 \times 10^{-5} \text{ mol l}^{-1}$, the total amount of TBZ extracted in 100 ml water as 0.394 mg. This amount obviously exceeds the provided maximum level of 6 mg/kg, by the current regulations in the case of citrus fruits

II.3. Conclusions

A complete theoretical and experimental vibrational Raman characterization of TBZ has been reported for the first time, allowing to study the vibrational properties in a broad range of concentrations and pH conditions. We have shown that TBZ can be rapidly detected by means of Raman (at millimole concentration level) and SERS spectroscopy (from micro- to picomole level) using Ag colloidal nanoparticles as enhancing substrate and a portable, compact, mini-Raman spectrometer. Different SERS behavior was found for TBZ dissolved in ethanol compared to aqueous solution, where the detection limit was three orders of magnitude lower. TBZ adsorbs on the Ag nanoparticles through the S and N atoms of the ring 1 and 2 resulting a standing up orientation when ethanol is used as solvent and in a tilted to parallel orientation with respect to the silver surface when dissolved in water, respectively. The protonated species supposed from the Raman spectra of aqueous solution revealed the new N-H bands at 1643 cm^{-1} and a slight shift in the specific skeletal vibrations. Vibrational data were employed to detect TBZ from treated citrus and bananas fruits samples using a simple approach of immersing them in water and performing SERS of the resulted solution. The identification of TBZ in neutral form was achieved by recording SERS spectra within 8 seconds acquisition time and comparing the signal with that of standard prepared samples. SERS signal of TBZ revealed specific bands intensity ratio I_{1389}/I_{484} as a function of concentration which allowed to rapid detect the TBZ concentration level in fruits.

A total amount of 0.394 mg TBZ was concluded in the water sample after 24 h immersing 5 g citrus peel, which results in an estimated value of 78 mg/kg, 13 times higher than the maximum allowed by current regulations. Based on the SERS signal comparison, higher TBZ content was found in orange, whereas the grapefruit, lemon and “bio” lemon revealed the same value; only banana fruit revealed the SERS ratio $r < 1$ suggesting lowest level, within the allowed limits. These results provided a fast, cheap and highly sensitive approach in monitoring thiabendazole in fruits. Further studies regarding the penetration depth of the TBZ in the fruit skin and the possibility to detect it using SERS are in progress.

III. Vibrational characterization and monitoring of some biotoxin in aquaculture products

III.1. Marine biotoxins

DA acid is the toxin responsible for amnesic shellfish poisoning (ASP). ASP is a new malady, entered the public health lexicon in 1987. [31] ASP symptoms include vomiting, nausea, diarrhea and abdominal cramps within 24 hours of investigation. In more severe cases, neurological symptoms develop within 48 hours and include headache, dizziness, confusion, disorientation, and loss of short memory, motor weakness, seizures, profuse respiratory, secretions, cardiac arrhythmias, coma and possibly death.

Both shellfish such as mussels, oysters, scallops, clams, limpet and fish can accumulate this toxin without apparent ill effects. In shellfish toxins mainly accumulate in the digestive glands, in fish accumulate in tissues.

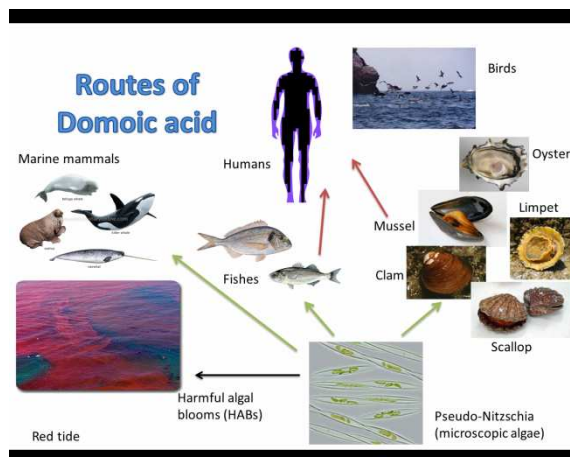


Fig.11. Rute of Domoic Acid

DA has also resulted in the mortality of hundreds of marine birds, mammals and fish at several other instances and locations in different parts of the world. (Fig.10)

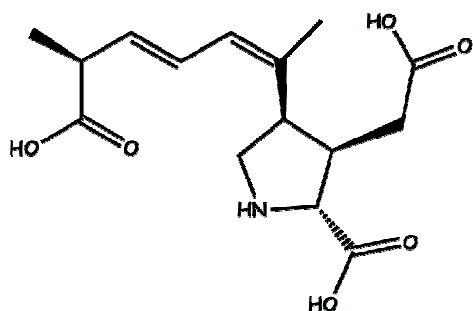
The European Union has established a permitted level of 20 mg DA/kg in shellfish. [32]

There are a number of ways to detect DA in algae and in food. These methods are very sensitive and can detect DA at levels

below those of concern in food. The low levels, which must be detectable, mandate prior separation of DA from many interfering substances in most currently, used chemical methods. These methods are expensive and time consuming and require complex sample preparation. Another possibility is the bioassay, what require the sacrifice of animals or the use of expensive reagents. Time is very important in detection of DA, because it can be found in perishable foods.

III.2. Domoic Acid

DA, $C_{15}H_{21}NO_6$, (molecular weight 311.3303 g/mol) is a naturally occurring excitatory neurotoxin amino acid produced by microscopic algae, specifically the diatom species *Pseudo-nitzschia*. It was first isolated from the benthic red seaweed *Chondria armata* (“domoi” in Japanese) and was named after it by Takemoto and Daigo, in the late 1950s. [33, 34]



Takemoto and Daigo [33, 34] elucidated the molecular structure of DA: it is a tribasic amino acid, related structurally to glutamic acid and containing a proline ring. The molecular structure is shown in the Fig.12.

Fig.12. The molecular structure of DA

III.2.1. Raman and SERS spectra of seawater

In Raman spectra of Adriatic seawater were detected two water peaks, H–O–H bending (1641 cm^{-1}) and O–H stretching ($3000\text{--}3800\text{ cm}^{-1}$) modes, and one sulfate ion peak, the S–O stretch (981 cm^{-1}). (Fig.13)

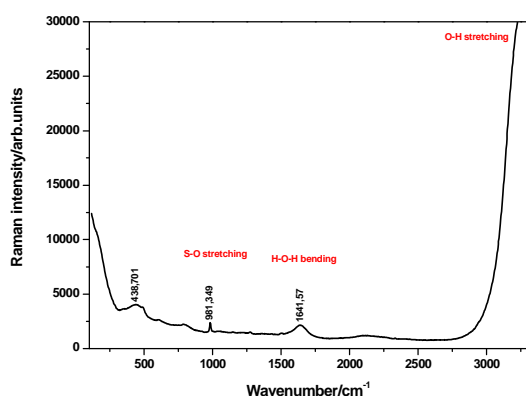


Fig.13. The Raman spectrum of seawater
Excitation: 532 nm; 20 spectrum, 15 sec, slit 100

There is a good correlation between the experimental values, obtained by measuring the Raman spectra of seawater, and the literature.

SERS signal of seawater (Fig.14) provide rich and complex information in a simultaneous manner, the presence of inorganic components (phosphate, nitrate, nitrite, ammonia, carbonates, sulfates) and organic species and organisms.

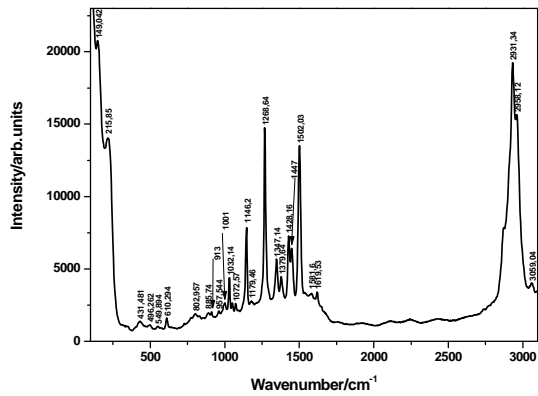


Fig.14. The SERS spectrum of seawater
Excitation: 532 nm; 10 spectrum, 3 sec, slit 50

SERS measurements show well resolved bands, narrow and precise, for collected "wild" seawater and for aquaculture water, without any chemical preparation of water samples, using a silver colloid for metallic substrate and a 3 seconds acquisition time.

SERS signal simultaneously displays information about the presence of nitrates, sulfates, ammonium ion, carbonates and phosphates as well as about salinity. The most significant SERS bands were observed at: 2958 cm⁻¹, 2931 cm⁻¹, 1502 cm⁻¹, 1269 cm⁻¹, 1146 cm⁻¹, 216 cm⁻¹. The presence of chlorides in SERS system is demonstrated by the observed band at 216 cm⁻¹, due to the newly formed bands (Ag-Cl) in SERS spectra. In comparison with the Raman spectra, the SERS signal of the seawater show significant differences in the bands positions and in the relative intensity of the bands, suggesting a strong chemisorption process. Theoretically, from the seawater can adsorb on the metal surface both organic and inorganic components.

III.2.2. The Raman spectrum of water from aquaculture

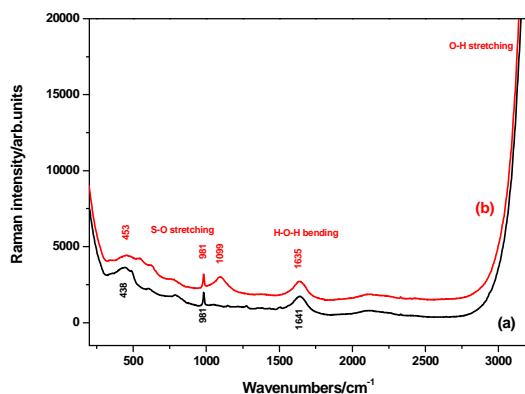


Fig.13. The Raman spectrum of seawater
Excitation: 532 nm; 20 spectrum, 15 sec, slit 100

The Fig.15. presents the Raman spectra of the aquaculture water in comparison with the Raman spectra of "wild" seawater, and the Fig. 16 present the SERS spectra of the both water.

The band at 438 cm⁻¹ in Raman spectra of seawater is shifted to the high wavenumber range at 453 cm⁻¹, while the band at 1641 cm⁻¹ is shifted to lower wavenumbers range at 1635 cm⁻¹ in the Raman spectra of aquaculture water. Appears a new

band in the case of aquaculture water at 1099 cm^{-1} , which has no counterpart in the Raman spectrum of the seawater. Compared to the Raman spectra of these two water samples reveal no significant differences for these analytical purposes.

There are significant differences in the SERS spectras of these two waters (*Fig.16*).

This SERS experiment clearly demonstrates the changes in the chemical composition of the water in the aquaculture area. The most intense bands were observed at 1363 cm^{-1} , 1508 cm^{-1} and 610 cm^{-1} . These spectra will be used as reference spectra for a possible detection of biotoxins in seawater.

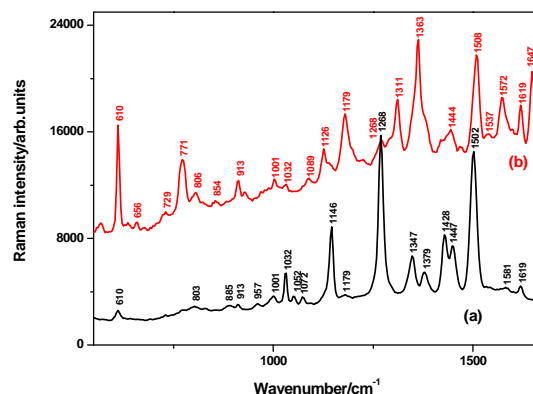


Fig.16. The SERS spectrum of (a) sea water in comparison with the spectrum of the(b) aquaculture water

III.2.3. The FT-Raman spectrum of domoic acid

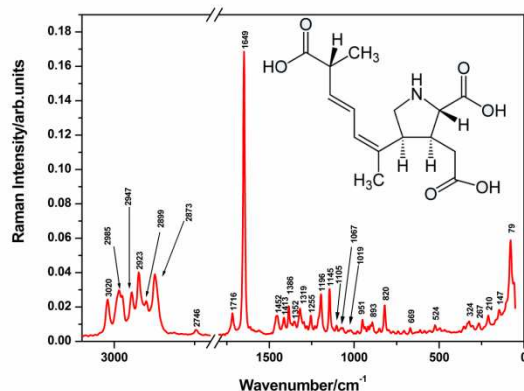


Figura.17. The FT-Raman spectrum of DA
Excitation: 1064 nm, putere 1 W, spectral resolution 2 cm^{-1} , 100 scans.

The FT-Raman spectra of DA solid, presented in *Fig.17.*, shows a most intense Raman band at 1649 cm^{-1} (theoretically 1650 cm^{-1}) [33] is assigned to the stretching vibration of the conjugated C=C double bond, which is characteristic of DA.

III.2.4. The SERS spectra of domoic acid

The SERS signal of the DA aqueous solution at $3.3 \cdot 10^{-4}\text{ mol l}^{-1}$ at pH 5.5 exhibits differences in band positions and relative intensities, when compared to the FT-Raman spectrum of solid DA (*Fig.18*), suggesting a strong chemisorption process on the Ag nanoparticles.

The presence of the SERS band at 223 cm^{-1} indicates the forming of the Ag-O [34] bond, with no counterpart for in the normal Raman spectrum. This is an indicative of the nearness of carbonyl group to the silver surface. Similar values are reported for the

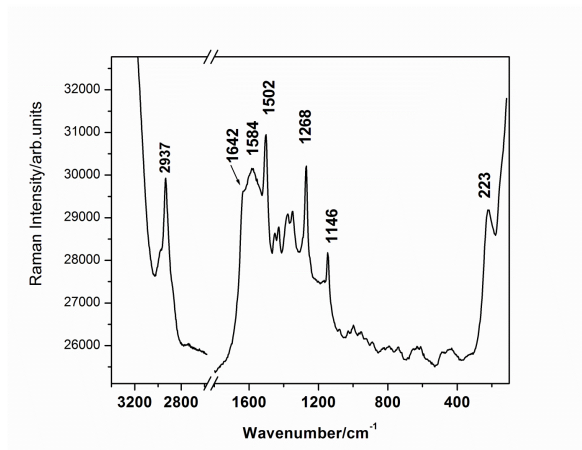


Fig.18. The SERS spectrum of DA in aqueous solution

wavenumbers assigned to $\nu(\text{Ag-O})$ SERS mode in literature.

Comparing to the normal FT-Raman spectrum the most prominent SERS band was observed at 1584 cm^{-1} .

The broadening of band assigned to C=C bond is likely due to a diverse set of molecular orientation, which is possible because DA has a conjugated double bond in the skeletal ring with three distinct carboxylic groups (COOH) at the molecule's periphery, and has also an imino group

(NH), vying to bind to the metal surface. [35-39]

Therefore, theoretically four possibilities exist, on which the molecule can interact with the metal surface. According to Falk et al. [40] DA exists in five distinct protonation states, whose proportion is strongly dependent on pH, where the imino >NH or the three carboxylate groups are sensitive in aqueous solutions. Taking into account that our stock DA solution has pH value of 5.5, where a single charged anion $-\text{COO}^-$ is present, the most probable adsorbed form would be through this functional group. Consequently we would expect to observe a new SERS band corresponding to the DA-Ag conjugates at about $216\text{-}222\text{ cm}^{-1}$. Indeed, in *Fig.18*, the strong band observed at 223 cm^{-1} confirmed our adsorption supposition.

III.2.4.1. Concentration dependence SERS spectra of DA in pure water and seawater

In order to probe the SERS capability for lower detection limit, several diluted DA seawater solutions were prepared from stock

In the case of seawater solution, an order of magnitude lower was achieved ($3.3 \times 10^{-8}\text{ mol l}^{-1}$).

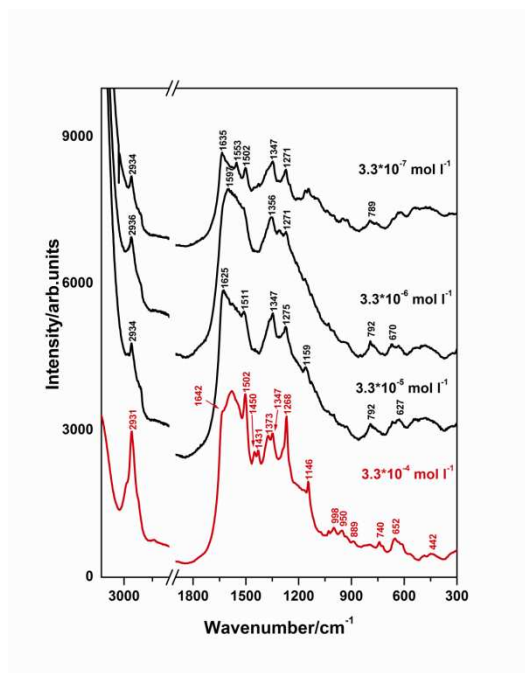


Fig.19. Concentration dependence SERS spectra of DA dissolved in pure water.

detectable at $2.5 \cdot 10^{-5} \text{ mol l}^{-1}$ ($7.8 \mu\text{g/ml}$). With the current SERS method we demonstrated the possibility to detect the DA in pure water solution at $3.3 \cdot 10^{-7} \text{ mol l}^{-1}$ ($0.1 \mu\text{g/ml}$), and in seawater solution at $3.3 \cdot 10^{-8}$ ($0.01 \mu\text{g/ml}$) mol l^{-1} . We reached a detection limit 78 times higher than previous SERS report, and even higher (780 times) when seawater was used as solvent.

III.2.4.2. SERS of DA on amino-functionalized Ag nanoparticles

In order to probe the capability of DA to bind to specific SERS tag, we employed 4-aminothiophenol (4-ATP) chemisorbed on Ag as a SERS label for detecting DA. It is well known that 4-ATP strongly interact with the Ag or Au nanostructure substrates and the Ag-ATP

Two distinct bands were observed also in the SERS spectrum of seawater at 1651 cm^{-1} and 1622 cm^{-1} at concentrations of less than $3.3 \cdot 10^{-5} \text{ mol}$ to $10^{-8} \text{ mol l}^{-1}$, while the bands at 1505 cm^{-1} and 1271 cm^{-1} are increased dramatically, suggesting an interaction with domoic acid and some seawater components, or a structural change of the molecule due to the different pH of seawater (7.5).

In seawater (Fig. 20), the high wavenumber range is completely dominated by seawater SERS signal (3600-1800 cm^{-1} range not given). A previous report on SERS on DA in aqueous solution shows that the toxin concentration was

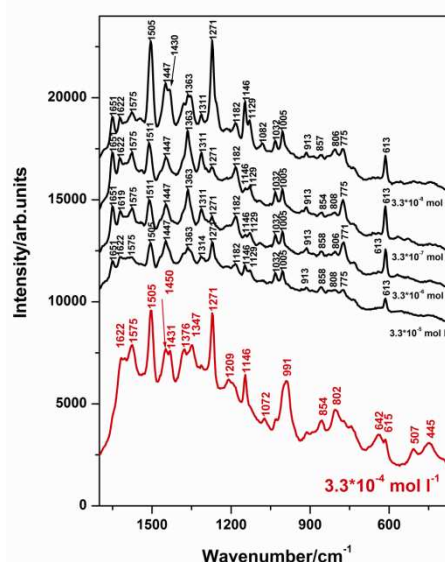


Fig.20. Concentration dependence SERS spectra of DA dissolved in seawater.

conjugates exhibits very strong SERS signals [39] of the chemisorbed ATP through the S atom, confirmed by the new SERS band of adsorbed ATP at about 212 cm^{-1} and assigned to Ag-S vibration mode.

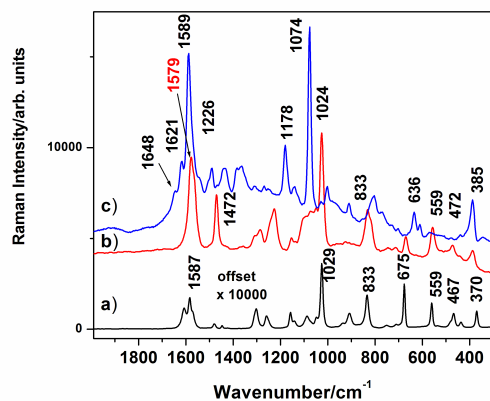


Figura.21. The FT-Ramanspectrum of 4-ATP pure (a), SERS of 4-ATP (b) SERS DA-AgNPs (c). Excitation: 1064 nm a); 532 nm b) și c).

Recent reports showed that p-ATP species could encounter photo changes in molecular identity due to the incident laser photons [41], resulting new chemical species formation, like p,p'-dimercaptoazobenzene, with totally different SERS signal. The new “b2 modes” at 1142, 1388 and 1432 cm^{-1} observed in the SERS spectra of ATP were actually assigned to p,p'-dimercaptoazobenzene when laser power applied was high (ca. 10 mW)

Taking into account specific environmental conditions to obtain a reproducible SERS signal from 4-ATP on Ag, we recorded SERS spectra in the case of DA solution dropped into the Ag-ATP SERS conjugated complex. Indeed, after intermediary SERS measurement of amino-AgNPs system (meaning laser exposure) and further adding DA solution results in less availability of the Ag-ATP conjugates to provide free amino-group, because of the laser induced photoreaction between neighbor ATP molecules generating p,p'-dimercaptoazobenzene on the Ag surface. In the case of chemical preparation of the SERS tag without laser exposure and intermediary signal collection, when further adding DA solution results in specific SERS due to the capped DA on the label.

The interaction of any carboxylate group with the amino-functionalized SERS labels is expected to be detectable as a change in the $1600\text{-}1700\text{ cm}^{-1}$ SERS range, where the amine bending (from ATP) and the carboxylate groups exhibit significant bands.

In SERS spectrum of 4-ATP absorbed on Ag surface, several very strong and medium bands were observed at 1079 cm^{-1} , 1176 cm^{-1} , 1597 cm^{-1} significantly depend on the

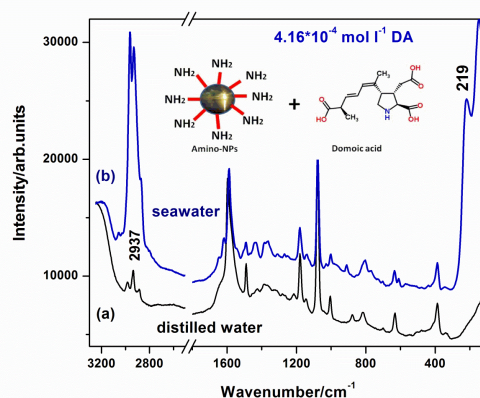


Fig.22. SERS spectru of DA dissolved in (a) distilled water, (b) in seawater on AgNPs

experimental conditions (high laser power generating photoproducts versus low laser power). The spectral range between 1600-1700 cm^{-1} is free of bands (*Fig.21*). To achieve molar ratios of 1:1 for ATP : DA we prepared an ATP SERS sample from 100 μl colloidal Ag and 10 μl 4-ATP ($4.5 \times 10^{-3} \text{ mol l}^{-1}$), and finally we added 50 μl DA aqueous solution (seawater solution respectively), at $10^{-3} \text{ mol l}^{-1}$ concentration. The SERS finally molar ratio was $C_{\text{DA}}/C_{4\text{-ATP}}=0.99$. We recorded FT-Raman spectrum of pure 4-ATP and compared to the corresponding SERS signal on Ag nanoparticles, to check the identity of the absorbed 4-ATP species (SERS label). Upon adding DA, SERS spectrum from the label revealed strong differences in the 1580 - 1700 cm^{-1} wavenumber range. The band at 1579 cm^{-1} is broadening and around 1648 cm^{-1} a prominent shoulder is observed.

The observed detailed differences suggested that the anchored DA on the 4-ATP functional groups were supposed to interact with the Raman label.

In seawater case (*Fig.22*), the large differences were observed. Appearance of new bands at 1645 cm^{-1} and 1617 cm^{-1} as well as in the low wavenumber range at 219 cm^{-1} and 149 cm^{-1} , demonstrated the possibility to identify the toxin species using the SERS specificity of the label. The specificity is raised not only from the margins of the spectral range, which is usually not well suited for portable equipments, but also in the fingerprint range, commonly used for Raman monitoring purpose.

III.2.4.3. SERS detection of domoic acid in fish tissue

Samples for SERS measurements were prepared by freezing a piece of at -20°C , and then placed in liquid nitrogen few minutes. For Raman microscopy mapping, the frozen samples were cut immediately to 40 μm thin sections with a microtome (Cryostat Frigocut 2800, at -25°C , and then deposited on a blade of CaF_2 Raman Microscopy (to avoid the fluorescence) and measured immediately.

The Raman spectrum of the fish sample is shown in *Fig. 23*. For the interpretation of Raman

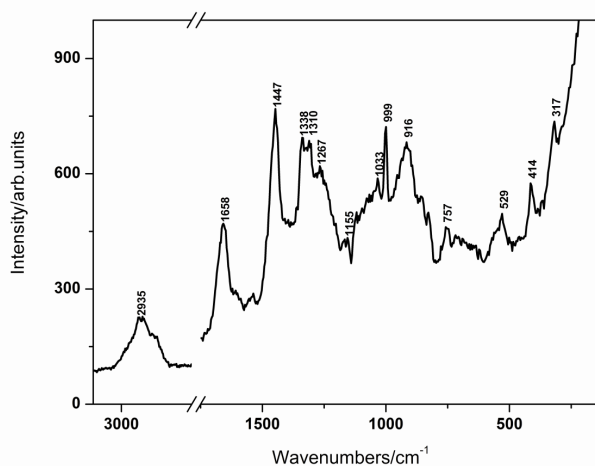


Fig.23. SERS spectrum of fish tissue

spectra, we used the comparison with a reference collagen spectrum, is abundant protein in all tissues of animal (and human).

It is noted that the specific protein bands, amide I (1658cm^{-1}) and amide III (1267cm^{-1}) and group-specific vibration CH_2 , $-\text{CH}_3$, of the 1447cm^{-1} , 2987cm^{-1} and 2935cm^{-1} as protein and lipid are unambiguously observed. Another characteristic band is observed at 1001cm^{-1} and generally attributed in literature with the stretching vibration of Phenyl ring from phenylalanine. The band at 317cm^{-1} is due to the CaF_2 substrate. Complex bands in the region $1300\text{-}1400\text{cm}^{-1}$ are assigned controversial attributed in literature, by some authors nucleic acids, as other authors hemic protein heme groups.

To fish tissue has added a few drops of domoic acid dissolved in pure water, and after a few minutes was measured in different depths. Averaged spectrum is shown in *Fig.24*

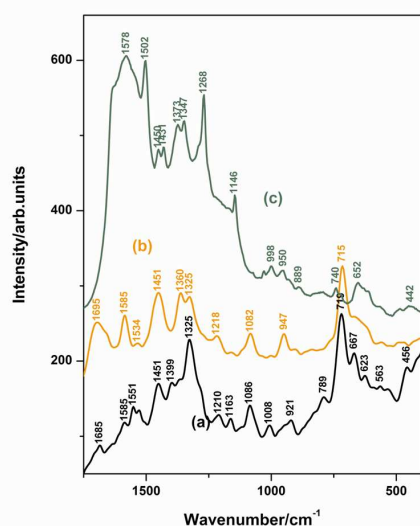


Fig.24. The SERS spectrum of fish tissue (a), with DA dissolved in pure water (b), SERS spectrum of DA dissolved in pure water (c),

The SERS spectrum of the tissue represents differences in the Raman signal, suggesting a strong incubation of the nanoparticles in the tissue, and respect a chemisorption process for some molecules in the structure of the tissue.

SERS spectrum of tissue DA shows a distinct spectral fingerprint.

Unambiguously observed SERS bands are characteristic of domoic acid (Fig. 24), which allows us to conclude that the SERS technique is able to detect and differentiate this biotoxin in fish

tissue. These results open new perspectives in the development of technology for current applications, the course will require database -specific SERS healthy tissues. Therefore the ideas developed in this thesis opens up new directions for applied research of current interest.

Conclusions

We obtained and characterized for the first time, the SERS signal of domoic acid both in pure water and seawater and have reached the limit of detection at a concentration of 0.33 nmol l⁻¹ (0.33 ppb) in distilled water , respectively 0.033 nmol l⁻¹ (0.033 ppb) in seawater, concentrations much lower than the accepted current regulations. Three different detection schemes of domoic acid (DA) in seawater are described, by dissolving the high crystalline sample by diluting the solution with pure water, seawater, or through the use of SERS -type markers Amino - AgNPs (as summarized in figure below)

Dependence of signal specificity of the method used has been discussed in all cases. To test the SERS technique and get high quality signal we used both pure nanoparticles and amino - functionalized. The concentration dependent SERS spectra revealed significant differences in adsorbed domoic acid signal strongly dependent on environmental conditions DA has been detected at a concentration of 4.16×10^{-4} mol l⁻¹ in the case of functionalized nanoparticles, a detection limit was of 5 orders of magnitude lower than that of pure Ag nanoparticle .

Using SERS to detect biotoxins demonstrate the ability to provide alternative ways to replace current methods costly and time-consuming analyzes of ongoing monitoring purposes It was demonstrated the orientation and the binding of domoic acid on the metal surface, and the detection of the toxins of marine seawater, using SERS at lower concentrations than currently used methods .

DA detection specificity amino - AgNPs is significant and unambiguous, not only to the spectral edge, but also within the so- called spectral " fingerprint " , which usually is very suitable for any portable Raman equipment. Therefore, the results provide valuable information for implementing a method implemented as a slight variation in situ, fast and cheap marine monitoring programs using portable and colloidal Ag nanoparticles .

REFERENCES (Selected)

1. http://www.fao.org/trade/docs/lcd-foodqual_en.htm
2. **A. Pinte**a, **C. Bele**, **S. Andrei**, **C. Socaciu**, *HPLC analysis of carotenoids in four varieties of *Calendula officinalis* L. flowers*, *Acta Biologica Szegediensis* 47, 37-40, (2003).
3. **T. Hodisana**, **C. Socaciu**, **I. Ropanb**, **G. Neamtu**, *Carotenoid composition of *Rosa canin* afruits determined by thin-layer chromatography and high-performance liquid chromatography*, *Journal of Pharmaceutical and Biomedical Analysis* 16, 521–528, (1997).
4. **A. Bunea**, **M. Andjelkovich**, **C. Socaciu**, **O. Bobisa**, **M. Neacsu**, **R. Verhéc**, **J. Van Camp**, *Total and individual carotenoids and phenolic acids content in fresh, refrigerated and processed spinach (*Spinacia oleracea*.)*, *Food Chemistry* 108, 649–656, (2008).
5. **T. Ilescu**, **S. Cîntă Pînzaru**, **D. Maniu**, **R. Grecu S. Aștilean**, *Aplicații ale Spectroscopiei vibraționale*, Casa cărții de știință, (2002), Cluj Napoca.
6. **S. Aștilean**, *Metode și tehnici moderne de spectroscopie optică, Spectroscopia IR și Raman*, Editura Casa Cărții de Știință, (2002), Cluj-Napoca.
7. **T. Ilescu**, **S. Cîntă Pînzaru**, *Specroscopia Raman și SERS cu aplicații în biologie și medicină*, Casa Cărții de Știință, (2011) Cluj-Napoca.
8. **W.E. Smith and G. Dent**, *Modern Raman Spectroscopy – A Practical Approach*, John Wiley&Sons, (2005).
9. **D. Bârcă-Gălățeanu**, **M. Giurgia**, **I. Iova**, **V. Sahini**, **A. Truția**, **R. Țițeica**, *Introducere în spectroscopia experimentală*, Editura Tehnică, (1966), București.
10. **Chalmers JM, Griffiths PR**. *Handbook of Vibrational Spectroscopy*, Wiley J&Sons, Chichester Baffins Lane, (2002), UK.
11. **J.A. Creighton**, *Spectroscopy of Surface*, R.J.H. Clark, R.E. Hester (Eds.), Wiley, (1988), New York.
12. **M. Moskovits**, **J.S. Suh**, *Surface selection rules for surface-enhanced Raman spectroscopy: calculations and application to the surface-enhanced Raman spectrum of phthalazine on silver*, *Journal of Physical Chemistry*. 88, 5526-5530, (1984).

13. **J.A. Creighton**, *Surface raman electromagnetic enhancement factors for molecules at the surface of small isolated metal spheres: The determination of adsorbate orientation from sers relative intensities*, *Surface Science* 124, 209-219, (1983).
14. **K. Kneipp**, *Surface-Enhanced Raman Scattering*, *Physics Today* 60, 40-47, (2007).
15. **A. Champion, P. Kambhampat**, *Surface-enhanced Raman scattering*, *Chemical Society Reviews* 27, 241-250, (1998).
16. **L. David, O. Cozar, C. Cristea, L. Gaina**, *Identificare structurii moleculare prin metode spectrosocopice*, *Presa Universitară Clujeană*, (2004), Cluj Napoca.
17. **T. Iliescu**, *Elemente de fizica laserilor și spectroscopie laser*, *Casa Cărții de Știință*, (2002), Cluj-Napoca.
18. **S. Cîntă-Pînzaru, A. Fălămaș, C. Dehelean, N. Leopold, C. Lehene, V. Chiș**, *Anti-tumoral betulin detection by surface enhanced Raman scattering*, *Studia UBB Physica*, 2, 25-33, (2010).
19. **A. Tao, F. Kim, C. Hess, J. Goldberger, R. He, Y. Sun, Y. Xia, P. Yang**, *Langmuir-blodgett silver nanowire monolayers for molecular sensing using surface-enhanced raman spectroscopy*, *Nano Letters* 3 1229-1233 (2003).
20. **T.Vo-Dinh**, *Surface-enhanced Raman spectroscopy using metallic nanostructures*, *Trends in analytical chemistry* 17(8-9), 557-582, (1998).
21. **A. Pîrnău**, Ph.D. Thesis, 18-19 (2007)
22. **P. Politzer, J. Murray**, *The fundamental nature and the role of the electrostatic potential in atoms and molecules*, *Theoretical Chemistry Accounts* 108, 134-142, (2002)
23. **J.J. Roothaan**, *New developments in molecular orbital theory*, *Reviews of modern physics*, 23, 63-68, (1951).
24. **F. Jensen**, *Introduction to Computational Chemistry*, John Wiley and Sons, (2001), New York.
25. **M. Saltmarsh**, *Essential Guide to Food Additives*, Leatherhead Food RA Publishing, (2000); 1-322.
26. **E. Oranescu**, *Aditivii alimentari, necesitate și risc*, Editura A.G.I.R., (2008), Bucuresti.
27. **C. Banu**, *Aditivi și ingrediente pentru industria alimentară*, Editura Tehnica, (2000) Bucuresti.
28. **M.S. Kim, M.K. Kim, C.J. Lee, Y.M. Jung**, *Bulletin of the Korean Chemical Society* 30, 1851-1854, (2009).

29. **Directiva 98/72/CE de modificare a Directivei 95/2/CE** privind aditivii alimentari alii decât coloranții și îndulcitorii, Jurnalul oficial al comunităților Europene, 04.11.1998, L295/18, 13/vol.27, pagina 117;
30. **E.C. Le Ru, S.A. Meyer, C. Artur, P.G. Etchegoin, J. Grand, P. Lang, F. Maurel**, *Experimental demonstration of surface selection rules for SERS on flat metallic surfaces*. Chemical Communications 47, 3903-3905, (2011).
31. **S.S. Bates, C.J. Boyd, R.K. Boyd, A.S.W. Freitas, M.Falk, R.A. Foxall, L.A.Hanic, W.D. Jamieson, A.W. McCulloch, P. Odense**: *Investigation on the source of domoic acid responsible for the outbreak of Amnesic shellfish poisoning (ASP) in eastern Prince Edward Island*. Atlantic Research Laboratory Technical Report 57, National Research Council, Canada, (1988)
32. **Regulation of the European Parliament and of the Council on the hygiene of foodstuffs**. Amended proposal for a regulation of the European Parliament and the Council laying down specific hygiene rules for food of animal origin (presented by the Commission pursuant to article 250(2) of the EC Treaty), Commission of the European Communities, Brussels, 27.1.2003
33. **Y. Djaoued, S. Balaji, S. Priya**, *Non-resonance micro-Raman spectroscopic studies on crystalline domoic acid and its aqueous solutions*, Spectrochimica Acta Part A, 67, 1362-1369, (2007).
34. **T. Takemoto, K. Daigo**, *On the constituents of Chondria armata and their pharmacological effect*, Archive for Pharmacy 293, 627-633, (1960)
35. **Q.Wu, W.H. Nelson, J.M. Treubing Jr., P.R. Brown, P. Hargraves, M. Kirs, M. Feld, R.Desari, R. Manoharan, E.B.Hanlon**, *UV Resonance Raman detection and quantitation of Domoic Acid in phytoplankton*, Analytical Chemistry, 72, 1666-1671, (2000).
36. **Y. Yao, W. H. Nelson, P. Hargraves, J. Zhang**, *UV Resonance Raman study of domoic Acid, a marine neurotoxic amino acid*, Applied spectroscopy 51, 785-791, (1997).
37. **Y. Djaoued, S. Balaji, S. Priya**, *Non-resonance micro-Raman spectroscopic studies on crystalline domoic acid and its aqueous solutions*, Spectrochimica Acta Part A, 67, 1362-1369, (2007).
38. **T. Takemoto, K. Daigo, Y. kondo, K. Kondo**, *Studies on the constituents of Chondria armata. VIII. On the structure of domoic acid* 86, Journal of pharmacological Society, 874-877, (1966).

39. **Y.F. Huang, D.Y. Wu, H.P. Zhu, L.B. Zhao, G.K. Liu**, *Surface-enhanced Raman spectroscopic study of p-aminothiophenol*, *Physical Chemistry Chemical Physics* 14, 8485-8497, (2012)
40. **M. Falk, J.A. Walter, P.W. Wiseman**, *Ultraviolet spectrum of domoic acid*, *Canadian Journal of Chemistry* 67, 1421-1425, (1989).
41. **T.Y. Olson, A.M. Schwartzberg, J.L. Liu, J.Z. Zhang**, *Raman and Surface Enhanced Raman Detection of Domoic Acid and Saxitoxin*, *Applied Spectroscopy* 65, 159-164, (2011).
42. **A. Doble**, *Pharmacology of Domoic Acid*, CRC Press, (2000).
43. **Y. Wang, S. Schlucker**, *Rational design and synthesis of SERS labels*, *Analyst* 138, 2224-2238, (2013).
44. **Y. Wu, L.B. Zhao, X.M. Liu, R. Huang, Y.F. Huang, B. Ran, Z.Q. Tian**, *Clean and modified substrates for direct detection of living cells by surface-enhanced Raman spectroscopy*, *Chemical Communications*. 47, 2520-2522, (2011).
45. **H. Chena, Y. Wanga, S. Donga, W. Wanga**, *Spectrochimica Acta, Part A: Molecular and biomolecular Spectroscopy* 64, 343-348, (2006).
46. **L. Skantarova, A. Orinak, R. Orinakova, F. Lofaj**, *4-Aminothiophenol Strong SERS Signal Enhancement at Electrodeposited Silver Surface*, *Nano-Micro Letters* 4, 184-188, (2012).
47. **E. Tan, P. Yin, T. You, L. Guo**, *Direct evidence for conversion of p-aminothiophenol to p,p'-dimercaptoazobenzene by in situ reduplicative surface-enhanced Raman scattering measurements*, *Journal of Raman Spectroscopy* 44, 1200-1203, (2013).

Publications list

ISI publications:

1. **Csilla Müller**, Leontin David, Vasile Chiş, Simona Cîntă Pînzaru, *Detection of thiabendazole applied on citrus fruits and bananas using surface enhanced Raman scattering*, Food Chemistry 145 (2014), 814-820.
2. **Csilla Müller**, Leontin David, Simona Cîntă Pînzaru, *Detection of thiabendazole applied to organic fruit by near infrared surface-enhanced Raman spectroscopy*, Spectroscopy Europe (Wiley), 25(4) (2013), 6-11
3. **Csilla Müller**, Karina Weber, Iva Pozniak, Jürgen Popp, Branko Glamuzina, Simona Cîntă Pînzaru, *SERS detection of domoic acid in seawater using pure or amino-functionalized Ag nanoparticles*, *Spectrochimica Acta Part A: Molecular and biomolecular spectroscopy*, submitted, under review since 23.07.2013
4. S. Cîntă Pînzaru, Iva Pozniak, M. Venter, **Csilla Müller**, Branko Glamuzina, *Assessing the new SERS-based sensing scheme for specific aquaculture environment monitoring of South-Eastern Croatian Coast, Fish and Fisheries*, (Wiley journal, impact factor 5.85) under review.

Acknowledgements

I would like to thank the entire staff of the Department of Biomedical Physics , Faculty of Physics, Babes-Bolyai University, for the support given to the achievement of this thesis.

My special gratitude is addressed to Prof. Dr. Leontin David, my head doctorate for support, encouragement and confidence and for the privilege and honor to achieve this doctoral work under their leadership .

I thank most especially Ms. Prof. Dr. Simona Cînta Pânzaru, who guided me constantly through research steps, because she gives me her experience and she revealed the secrets of the beautiful research field, vibrational spectroscopy .

I also want to extend my thanks and gratitude to selected Prof. Dr. Vasile Chiş, for important suggestions, guidance and scientific additions and also the timeliness and depth of advice given .

I would like to thank the entire staff of the Friedrich- Schiller University, IPHT, Jena, Germany, and especially to Prof. Dr. Jürgen Popp for professional and financial support for the realization of this thesis.

Not least, I wish to thank to the most important people in my life, my husband Ferencz, my parents and my sister, who were with me the whole time and gave unconditional support and love.

This work was made possible through financial support provided by the Sectoral Operational Programme Human Resources Development 2007-2013, co-financed by the European Social Fund, the project POSDRU/107/1.5/S/76841 with the title " Modern Doctoral Studies : Internationalization and Interdisciplinarity " .